0013-7227/05/$15.00/0
Printed in U.S.A.

Endocrinology 146(9):4042–4053

doi: 10.1210/en.2005-0020

Orexin A Modulates Mitral Cell Activity in the Rat Olfactory Bulb: Patch-Clamp Study on Slices and Immunocytochemical Localization of Orexin Receptors

Alexandre B. Hardy, Josiane Aïoun, Christine Baly, Karyn A. Julliard, Monique Caillol, Roland Salesse, and Patricia Duchamp-Viret

Laboratoire de Neurosciences et Systèmes Sensoriels (A.B.H., K.A.J., P.D.-V.), Centre National de la Recherche Scientifique, Unité Mixte de Recherche 5020, Université Claude Bernard, 69366 Lyon cedex 07; and Laboratoire Neurobiologie de l'Olfaction et Prise Alimentaire (J.A., C.B., M.C., R.S.), Equipe Récepteurs et Communication Chimique, Institut National de la Recherche Agronomique, 78352 Jouy-en-Josas, France

Orexin A and B are involved in feeding behaviors, and recently fibers containing these peptides were found in the rat olfactory bulb. These fibers, which originate from the lateral and posterior hypothalamus and the perifornical area, are distributed in the glomerular, mitral cell, and granule cell layers. Orexin receptors are mainly expressed by mitral cells. In the present study, RT-PCR experiments were done to determine orexin receptor expression during the early postnatal life of rats, and immunocytochemical experiments were performed to further clarify the structural and ultrastructural localization of orexin receptors in the olfactory bulb. Furthermore, a functional electrophysiological approach examined the action of orexin A on mitral cell excitability and spontaneous activity using *in vitro* patch-clamp techniques. RT-PCR results show that mRNA of the two type receptors, type 1 orexin receptors and type 2 orexin receptors, are expressed in the olfactory bulb of rat from 10 d to the adult stage. At the same ages, immunocytochemical data show that orexin 1 receptors are localized in the cell bodies of periglomerular, mitral/tufted, and granule cells. Immunoreactivity was also demonstrated in mitral/tufted cell dendrites arborizing in the glomerulus and mitral/tufted and granule cell processes running in the external plexiform layer. Functionally, orexin A produced either a direct, tetrodotoxin-insensitive depolarization in one group of mitral cells (7%), or, in another group (30%), an indirect, tetrodotoxin-sensitive hyperpolarization. Both actions were mediated by type 1 orexin receptors because the response was antagonized by SB-334867-A, a selective antagonist. Mitral cell recordings performed under bicuculline [γ-aminobutyric acid $(GABA)_A$ receptor antagonist], indicate that the orexin-induced indirect hyperpolarization was partly mediated through $GABA_A$ receptors. Because granule cells and periglomerular cells express orexin receptors and are GABAergic cells, they could be both involved in this hyperpolarization. Other mechanisms, which could support an indirect hyperpolarization of mitral cells through dopamine interneuron solicitation, are proposed. Our results provide data that should allow us to better understand neural communication and regulation mechanisms between the hypothalamic feeding centers and the olfactory bulb. (*Endocrinology* 146: 4042–4053, 2005)

MANY ANIMAL BEHAVIORS are triggered by odorant cues from the environment, and in particular, food odors are among the major determinants for food choice and food learning. It has been clear for several years that the olfactory system is involved in feeding behavior. The nutritional status of the animal was shown to influence reactivity to food odors of mitral cells; the main output neurons of the olfactory bulb (1–5). For example, it had been demonstrated that in fasted rats, 70% of mitral cells were stimulated by food odor stimulation *vs.* 12% for a nonfood odor, whereas in fed animals only 11% responded to food odors (6).

First Published Online June 23, 2005

Abbreviations: ACSF, Artificial cerebrospinal fluid; DAB, diaminobenzidine; EPL, external plexiform layer; EPSP, excitatory postsynaptic potential; GABA, γ-aminobutyric acid; GABAergic, neurons that use GABA as neurotransmitter; GAPDH, glyceraldehyde-3-phophate dehydrogenase; HYPO, hypothalamus; OB, olfactory bulb; ORX1, orexin receptor 1; ORX2, orexin receptor 2; OX, orexin; OXA, orexin A; OXB, orexin B; P, postnatal day; PG, periglomerular cell; RT, room temperature; TTX, tetrodotoxin.

***Endocrinology* is published monthly by The Endocrine Society (http://www.endo-society.org), the foremost professional society serving the endocrine community.**

Conversely, it was shown that odors regulate food intake behavior. Indeed, Le Magnen (7) showed that rats increased their food intake if, once satiated, they were presented with differently odorized foods. Moreover, it is an everyday experience for humans and animals that food odors are attractive before feeding, whereas the same stimuli may become neutral or even aversive after feeding. Sensory olfactory inputs are thus crucial in nutrition behavior of humans and animals. Olfactory system involvement begins with the food search step because olfactory sensitivity levels provide the signal detection that allows the animals to follow the concentration gradient toward the food source. Then the olfactory system contributes to the palatability analysis of the food; the appetence of the animal for food is defined by its internal physiological status.

Hypothalamic feeding centers (8) analyze metabolic cues and in turn regulate the appetite. These centers send direct and specific projections to olfactory structures, especially on the olfactory bulb (OB), the first integrative relay of the system (9–13). The discovery of orexin A (OXA) and B (OXB) or hypocretin I and II (11, 13), two peptides derived from the same prepropeptide and contained in neurons localized in

the lateral hypothalamus and perifornical area, provided new insights into the regulation mechanisms of feeding. Orexin (OX) neurons in the lateral hypothalamus and perifornical area are controlled by changes in circulating nutriment because they are activated by natural hypoglycemic conditions (14) or insulin-induced ones (15), whereas they are inhibited by glucose and signals related to the ingestion of food (15–19). These data led to the classification of OX neurons of the lateral hypothalamus and perifornical area as glucose-sensitive neurons (20). Furthermore, OX neurons are stimulated by an increase of circulating lipids. Thus, OX neurons are negatively related to the glucose level but inversely related to circulating fat (21), the latter relation suggesting a role of this peptide in the increased activity associated with a high-fat diet (22, 23).

The majority of physiological studies (for reviews see Refs. 24 and 25) indicate that orexins are potent stimulators of food intake (26, 27), with OXA being more effective than OXB. Moreover these peptides interact with various neuronal pathways to potentiate apparently divergent functions (for review see Ref. 28). Currently two closely related G protein-coupled receptor types termed type 1 orexin receptors (ORX1) and type 2 orexin receptors (ORX2) have been identified. Although OXA has the same affinity for ORX1 and ORX2, OXB has a 10-fold greater affinity for ORX2 (13, 29, 30).

Caillol *et al.* (31) demonstrated that in the OB, immunoreactive OXA varicose fibers were mainly around glomeruli, in mitral cell and granule cell layers. Glomeruli are spherical neuropiles lying at the OB periphery in which primary axons synapse with mitral cells; they are delimited by GABAergic interneurons called periglomerular cells. Granule cells are deep GABAergic inhibitory interneurons. The localization of OXB labeling paralleled that of OXA. However, immunoreactivity to ORX1 and ORX2 were detected only in some mitral/tufted cell bodies, ORX2 labeling being very faint (31). This localization may support, at least partly, data reporting that OB mitral cell reactivity to odors was modulated according to hunger and satiation states in rats (3).

Our exploration of OX actions on the OB network should provide a better understanding of the cross-talk between olfactory and metabolic cues in the brain, as being at the basis of nutritional behavior. This study analyzed specifically OX action on mitral cells, its putative cell targets in the OB (31), through an *in vitro* patch-clamp study. To do so, the actions of OXA and SB-334867-A (ORX1 antagonist; GlaxoSmith-Kline, Harlow, Essex, UK) were tested on the spontaneous activity and excitability of mitral cells. Furthermore, an immunocytochemical study was done to clarify cellular and subcellular localizations of ORX1, the most expressed orexin receptor in the OB. In addition, because no data are available on the early ontogenetic development of orexin innervation and orexin receptors in the OB and because electrophysiological studies on slices were performed on 10- to 25-d-old-rats, the presence of ORX1 was evaluated through RT-PCR experiments on rats and adults that were 10–25 postnatal days (P) old. Altogether, the data are expected to provide some enlightenment about the neurochemical modulatory effect of OXA on OB activity and to reveal what cell types of the bulbar network are the targets of orexin innervations. Furthermore, this first functional study is expected to give rise to preliminary hypotheses dealing with the role of the olfactory system in the regulation of food-intake processes.

Materials and Methods

All experiments were done according to the European Communities Council Directive of 24 November 1986 (86/609/EEC).

RT-PCR analysis of orexin receptor expression in the hypothalamus (HYPO) and OB

Animals and tissue preparation. Experimental procedures were carried out to minimize animal suffering and the number of rats used. Male Wistar rats from our own breeding stock were housed in 12-h light, 12-h dark cycles with free access to food and water. A total of three animals were killed by decapitation at 10 d, 25 d (P10–P25), and 2 months (adults). Before weaning (P21), young were kept with the dam. The brain was quickly removed and the HYPO and OB was dissected on ice.

Total RNA isolation and RT-PCR analysis. Total RNA was isolated from the HYPO and OB using the guanidium-thiocyanate-phenol-chloroform extraction method (32), and DNase I-treated (Roche Molecular Biochemicals, Meylan, France) cDNA was reverse transcribed from 3 μg total RNA by 50 U Superscript II reverse transcriptase according to the manufacturer's procedures (Life Technologies, Inc.-BRL, Cergy Pontoise, France). A control reaction omitting the enzyme was systematically included to confirm the absence of genomic contamination. An internal standard using glyceraldehyde-3-phophate dehydrogenase (GAPDH) as a referent housekeeping gene was systematically included. For PCR amplification, a 1-μl reverse transcription aliquot was added to 20 μl of a reaction mixture containing each pair of primers: GAPDH primers, up 5′-AAACCCATCACCATCTTCCA (1057–1077 on NM_017008), low 5′-AGGGGCCATCCACAGTCTTCT (1417–1397); ORX1 primers, up 5′-CCTGCCTCCAGACTATGAGGA (631–651 on NM_013064), low 5′-ATCTTAGGGTAGAGTTCATCT (1206–1186); ORX2 primers, up 5′-GATTCCCTCCCTCGTCGCAA (81–100 on NM_013074.1) and low 5′-CAGCGTTCATCGCAGACTGTA (700–681).

PCRs were done according to standard procedures using 0.5U Taq DNA-polymerase (Promega, Charbonnieres, France). A thermal cycler apparatus was used in the following conditions: 45 sec at 94 C, 45 sec at 57 C, and 45 sec at 72 C for 23 (GAPDH) or 35 cycles (ORX1 and ORX2). PCR products (3 μl aliquot) were resolved on 1.5% of agarose gel in 1× TAE (Tris-acetate-EDTA) buffer containing 1 μg/ml of ethidium bromide. A molecular-weight-marker was systematically included (1 kb DNA ladder, Life Technologies, Inc., InVitrogen, Cergy-Pontoise, France). Gels were photographed under UV light. OB PCR products from 25-d-old rats were sequenced (Genome Express, Paris, France) and then analyzed using BLAST programs.

Structural and ultrastructural immunocytochemical study

Seven male Wistar rats were used for light microscopy: three adults rats (2 month old, body weight 300 g), two P10 and two P25. Animals were deeply anesthetized (pentobarbital 60 mg/kg body weight, ip, Sanofi, Paris, France) and perfused transcardially with 100 ml saline and then with 150 ml of a freshly prepared fixative solution of 4% paraformaldehyde in 0.1 M PBS. The olfactory bulbs were carefully dissected and postfixed in the same fixative for 3 h at room temperature, cryoprotected with saccharose (30%), and cut in a cryostat in serial coronal sections (14 μm thick). Sections were first treated for 30 min at 4 C in 0.5% H_2O_2 in PBS to eliminate endogenous peroxidases and then carefully washed. A 1-h immersion in a solution of 10% normal goat serum in PBS at room temperature (RT) was used to block nonspecific sites. Sections were then incubated, at 4 C for 3 d, in the primary antibody diluted 1/2000 in PBS containing 1% normal goat serum, 0.025% Triton X-100, and 0.1% BSA (rabbit antiserum directed against rat/human ORX1; Alpha Diagnostic International, Cortec, France). As controls some sections were incubated without the primary antibody. After several washings in PBS containing 1% nonfat freeze-dried milk, sections were incubated in biotinylated goat antirabbit IgG (Vectastain Elite kit, Vector Laboratories, Burlingame, CA) in the same buffer for 1–2 h at RT. All

sections were then rinsed in PBS and incubated for 1 h at RT in either an avidin-biotin peroxidase complex (Vectastain Elite kit), with the labeling then visualized using 3, 3′-diaminobenzidine tetrahydrochloride solution intensified by nickel (peroxidase substrate kit, Vector Laboratories), or in streptavidin fluorescein (1:1000, Vector Laboratories); 4′,6′-diamino-2-phenylindole (DAPI) was added for 10 min (1:10,000 in PBS) to achieve a nuclear counterstaining.

Electron microscopy was done on three adult male Wistar rats that were deeply anesthetized as described above. They were transcardially perfused with 200 ml saline, followed by 300 ml of a freshly prepared fixative solution (paraformaldehyde 4%, picric acid 0.2%, and glutaraldehyde 0.125% in 0.1 M phosphate buffer). The brains were dissected and postfixed overnight at 4 C in the same fixative. Serial coronal sections (50 μm) were obtained with a vibratome (VT1000S, Leica, Nussloch, Germany) and collected in phosphate buffer. The immunocytochemical study was performed on free-floating sections in PBS using a preembedding protocol, as previously described, except that Triton X-100 was omitted and sections were immersed in 1% sodium borohydride ($NaBH_4$, Sigma-Aldrich, Saint Quentin Fallavier, France) in PBS to quench free aldehydic sites before blocking nonspecific sites.

The ORX1 was visualized using the diaminobenzidine (DAB) method adapted for electron microscopy. Sections were washed in 0.05 M sucrosed Tris buffer (pH 7.6) and then incubated in a 0.05% DAB substrate in presence of H_2O_2. The reaction was conducted under a stereomicroscope and stopped by immersion of the sections in Tris buffer. The most immunostained sections were selected, osmicated in a 1% OsO_4 solution, stained en bloc with 1% uranyl acetate, dehydrated in a graded series of ethanol, and embedded in Epoxy resin (LX112, Ladd Research Industries, Inland Europe, Conflans/Lanterne, France). Semithin sections (1–2 μm) were obtained from resin-embedded material and stained or not with toluidine blue. Ultrathin sections (50–100 nm) were collected on copper grids, contrasted with lead citrate, and observed with a Philips (Suresne, France) CM12 electron microscope under an 80-kV accelerating voltage.

Patch-clamp recording experiments

Slice preparation. Experiments were performed on 10- to 25-d-old rats (Wistar). Animals were killed by decapitation and the head was quickly immersed in ice-cold artificial cerebrospinal fluid (ACSF, 2–4 C) containing (in millimoles) 125 NaCl, 4 KCl, 25 $NaHCO_3$, 2 $CaCl_2$, 1.25 NaH_2PO_4, and 1 $MgCl_2$ (pH 7.3) when bubbled with a mixture of 95% O_2 and 5% CO_2; the osmolarity was adjusted to 320 mOsm with glucose. The OB was then removed as previously detailed (33) and cut in sagittal or horizontal slices (250–350 μm thick) using a vibratome. Slices were incubated in a Gibb's chamber at 30 C for 1 h and then stored at RT. For electrophysiological recordings, slices were transferred into the experimental chamber (2 ml) mounted on an upright microscope (Axioscope FS, Zeiss, Göttingen, Germany). During recordings, slices were continuously perfused with oxygenated 30 C ACSF at a 2.5 ml/min rate. Neurons were visualized using a water-immersion ×40 objective with differential interference contrast optics (Nomarski, Edgewater, NJ) or through infrared illumination (Hamamatsu camera; Hamamatsu Photonics France, Massy, France).

Electrophysiological recordings. The whole-cell recording technique was used. Patch pipettes were pulled from borosilicate glass (outer diameter 1.5 mm; inner diameter 1.17 mm, Clark electromedical instrument from Phymep, Paris, France) without internal filament and were not fired polished. Recording pipettes had a tip resistance of 2–4 MΩ. Seal resistance was always greater than 3 GΩ. The recording pipette solution contained (in millimoles): 121.4 $KMeSO_4$, 13.6 KCl, 4 $ATPNa^+$, 0.1 $GTPNa^+$, 10 HEPES, 1 $MgCl_2$; pH was set to 7.4 with NaOH and osmolarity to 310 mOsmol with glucose. For all experiments, the reported values of membrane potential are the values after correction for the junction potential.

A bipolar concentric electrode was placed in the olfactory nerve layer near the recorded mitral/tufted cell to stimulate the olfactory nerve. Monophasic square pulses were then delivered through a stimulus isolation unit.

Voltage and current measurements of neuron activity were performed with an axoclamp 2B amplifier (Axon Instruments, Foster City, CA). All experiments were controlled by a PC-pentium III computer using 12 bit A/D-D/A converters (digidata 1200B, Axon Instruments; sampling frequency 30 KHz) and the clampex software (version 8.1). All data are presented as the mean ± SD.

OXA (Bachem, Voisins-le-Brettoneux, France) was aliquoted and stored at −20 C. OXA action on mitral cells was tested by switching the ACSF solution for 1 min to one containing OXA (10–200 nM; see Refs. 34–36). All solutions perfused the tissue at 2.5 ml/min. Some experiments were performed in the presence of tetrodotoxin (TTX, 1 μM, Tocris, Fisher Bioblock Scientific, Illkirch, France), which blocks the voltage-gated sodium channels. Picrotoxin (50 μM, Sigma) and bicuculline (10 μM, Sigma) were also used to block chloride conductance and $GABA_A$ receptors, respectively. ORX1 was blocked by SB-334867-A (10 μM; GlaxoSmithKline; see Refs. 30, 37, and 38).

Results

RT-PCR analysis of orexin receptor expression in the OB

RT-PCR of OB samples revealed a single band of the expected size and sequence for both ORX1 (556 bp) and ORX2 (620 bp) mRNAs, attesting to the presence of these mRNAs in the OB of rats aged 10 and 25 d and 2 months (Fig. 1). The relative abundance of both ORX1 and ORX2 mRNAs seemed to be lower in the OB, compared with the HYPO, because the GAPDH gene was equally amplified as a 361-bp fragment in both tissues. Albeit nonquantitative, the levels of both receptors mRNA did not dramatically change during development.

Structural and ultrastructural immunocytochemical study

Light microscopic localization of ORX1 immunoreactivity in the OB. Because Caillol *et al.* (31) showed that ORX1 seems expressed at higher levels than ORX2 at the protein level, the present study focused on ORX1. Our observations confirmed and refined previous description of ORX1 localization in the OB (31). At light microscopic level, ORX1 immunoreactive

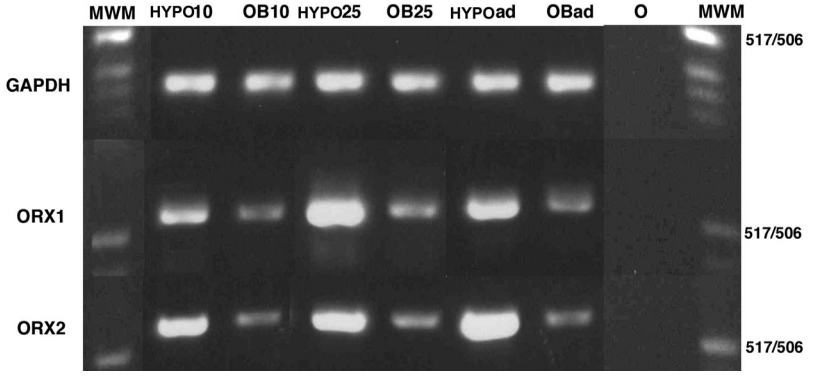

FIG. 1. Detection of different orexin receptors mRNA by RT-PCR analysis in HYPO and OB tissues. PCR products for GAPDH, ORX1, and ORX2 were obtained from HYPO or OB samples of 10- or 25-d-old (10–25) or adult rats (ad) and run on an ethidium bromide-stained-1.5% agarose gel. Products are of the expected size and were controlled by sequencing the PCR products derived from OB25 samples. O, Control without DNA matrix; MWM, molecular weight marker, 1 kb DNA ladder (only the 512/506-bp band is specified). Only one representative rat for each experimental point is shown (n = 3 for each).

cells were identified by a dark staining due to the presence of the DAB-nickel reaction product or by green fluorescence in their cytoplasm (Fig. 2F). In P10, P25, and adult rats, ORX1 was distributed with a laminar pattern. ORX1 immunoreactivity was obvious in cell bodies in the glomerular (Fig. 2, A, B, and E), mitral cell, and granule cell layers (Fig. 2, C–F). The immunolabeling was not homogeneous along the mitral cell layer: immunoreactive mitral cells were clustered in patches. In the same way, some glomeruli were ORX1 immunoreactive, whereas others were devoid of immunolabeling. Most often ORX1 immunoreactive glomeruli were located above the immunoreactive zones of the mitral cell layer. In the glomerular layer, most of the immunoreactive cell bodies were found at the base of the glomerulus, just above the external plexiform layer. Some of these neurons were rather elongated in shape, whereas the others were slightly smaller and round. Some of these round neurons were also observed around the glomerulus. According to their location, these neurons could correspond to external tufted cells and periglomerular cells (PGs), respectively. In semifine sections, brown dots probably corresponding to mitral cell dendrites appeared dispersed in the external plexiform layer (EPL) and inside glomeruli. In sections in which the primary antiserum has been omitted, no immunolabeling was observed.

Ultrastructural localization of ORX1 immunoreactivity in the OB. Electron microscopy observations confirmed the light microscopy observations. At the ultrastrutural level, the presence of ORX1 was visualized by electron-dense DAB deposits. The identification of the immunoreactive elements was based on the descriptions of Pinching and Powell (39, 40) and Price and Powell (41).

Deep in the OB, ORX1 were expressed in granule cell bodies in which they were localized both in the cytoplasm and in the neighborhood of the plasma membrane (Fig. 3A). In the mitral cell layer, rather few mitral cell bodies (characterized by their typical and abundant stacks of rough endoplasmic reticulum) were ORX1 labeled. However, in ORX1 immunoreactive mitral cells, labeling was obvious and consisted of numerous patches localized both between cisternae of endoplasmic reticulum and in the neighborhood of the plasma membrane, indicating that ORX1 is locally synthesized and folded at membrane (Fig. 3B). In the EPL, immunolabeling was shown in mitral cell and granule cell dendrites (Fig 3C) and reciprocal synapses between ORX1 immunoreactive mitral cells, and granule cell dendrites could be observed (Fig. 3D); the accumulation of labeling near the synapse should be noted.

In the glomerular layer, immunolabeling was found both

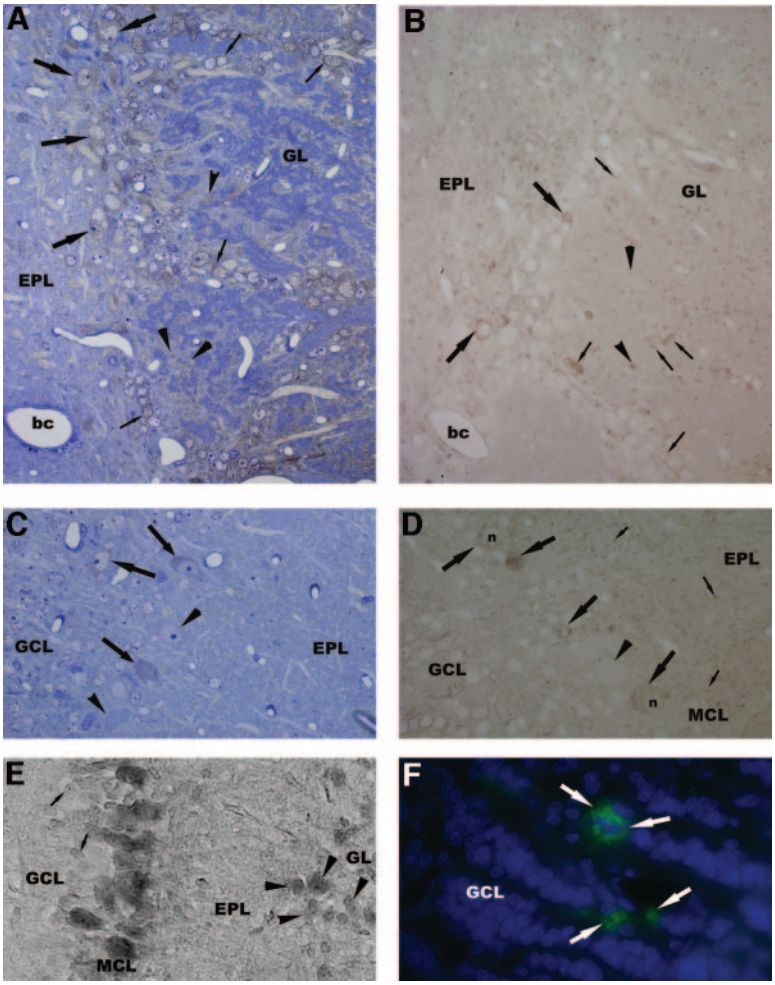

FIG. 2. Light microscopic localization of ORX1 immunoreactivity in the OB. The presence of ORX1 in the OB was checked on semithin sections obtained from 50-μm sections embedded in epoxy resin (adults, A–D) and on thin sections (14 μm) (P10 rat, E; P25 rat, F). The semithin sections were observed either stained with Toluidine blue (1 μm thick, A and C) or without any counterstaining (2 μm thick, B and D). The presence of ORX1 was visualized by a dark DAB (A–D) or DAB-nickel staining spread in the cytoplasm of immunoreactive (ir) cells (E) or a green fluorescence (F; *blue staining*: 4′,6′-diamino-2-phenylindole nuclear coloration). ORX1 ir-cell bodies were identified in all layers, except the olfactory nerve layer. In the glomerular layer (A and B, ×40 immersion), ir-cell bodies were observed around the glomeruli. Large elongated cell bodies mostly located at the basis of the glomeruli could be external tufted cell (*large arrows*), whereas small round cell bodies on the border could be identified as PG cells (*thin arrows*). Inside the glomeruli, *brown dots* are likely mitral cells dendrites (*arrowheads*). In the mitral cell layer, the cytoplasm of some mitral cells was highly ir (*large arrows*, C and D, ×40 immersion). Some mitral cells did not express ORX1 (*arrowheads*, C and D). In some sections the mitral cell nucleus was apparent and devoid of immunolabeling (C and D). Some granule cells were ORX1-ir (E and F). In the EPL a punctiform DAB-labeling (*thin arrows* in 2D) corresponded presumably to mitral cell dendrites. bc, Blood capillary; GCL, granular cell layer; GL, glomeruli; MCL, mitral cell layer; n, nucleus.

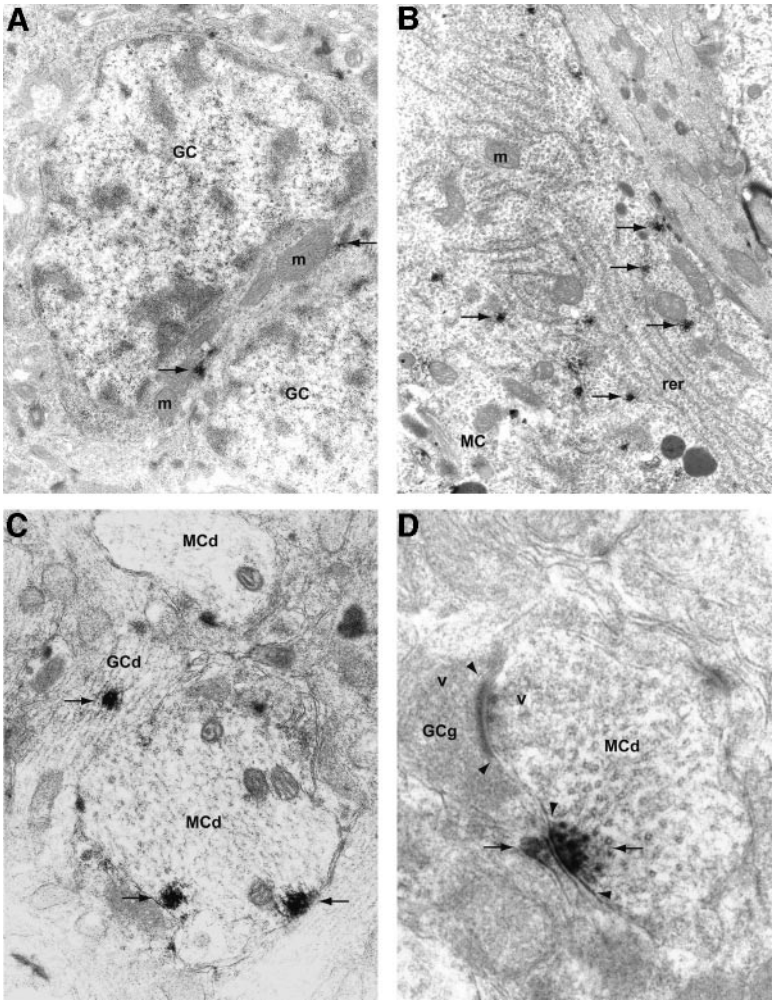

FIG. 3. Ultrastructural localization of ORX1 in the granule cell layer, mitral cell layer, and EPL of the OB. At the ultrastructural level, the presence of ORX1 was visualized by electron-dense DAB deposits (*arrows*). In the granule cell layer (A, ×10,500), ORX1 immunoreactivity was identified in numerous granule cell bodies. Labeling is either cytoplasmic or very close to the plasma membrane. In the mitral cell layer (B, ×11,000), some mitral cells exhibited a punctuated labeling, which is also both cytoplasmic and close to the plasma membrane. In the EPL (C, ×7000), ORX1 immunoreactivity was found in mitral cell and granule cell dendrites. In some cases (D, ×17,500), ORX1 immunoreactive gemmules of the granule cell were observed establishing synaptic contact with mitral cell dendrites through reciprocal synapses (*arrowheads*). rer, Rough endoplasmic reticulum; GCg, gemmule of granule cell; GC, granule cell; m, mitochondria; MCd, mitral cell dendrite, MC, mitral cell; GCd, granule cell dendrite; v, synaptic vesicle.

in cell bodies and processes. Some ORX1 immunoreactive neurons observed at the periphery of the glomeruli were small round cells almost completely filled with their nuclei, surrounded by a thin rim of cytoplasm (Fig. 4A). These ultrastructural features corresponded to those of PGs. At the base of the glomerulus (infraglomerular area), some immunoreactive neurons were identified. They were slightly larger than PGs; their cytoplasm was more abundant and showed a well-developed granular endoplasmic reticulum (Fig. 4B). On the basis of the description of Pinching and Powell (40), these neurons were identified as external tufted cells. The glomerular neuropil showed numerous ORX1 immunoreactive processes. Strongly immunoreactive dendritic shafts were observed. Given the regular arrangement of their neurotubules, they were identified as the main dendritic shafts of tufted cells (not shown). Numerous dendrites of mitral/tufted cells, surrounded by olfactory neurons terminals, were ORX1 immunoreactive (Fig. 4, C and D). Some gemmules of PG were also ORX1 immunoreactive (Fig. 4E). In the glomerular neuropil, the terminals of the olfactory axons were never ORX1 immunoreactive.

Patch-clamp recording experiments

Whole-cell recordings were obtained from 204 mitral cells that were strictly located in mitral cell layer. Cell identification was based on location, electrophysiological properties, morphology, and size. Mitral cells showed an average resting potential of -60 ± 4 mV and a mean input resistance of 74 ± 38 MΩ.

Among the 204 mitral cells, 61 (30%) were responsive to OXA. In current clamp mode, bath application of OXA induced a hyperpolarization (n = 46; 23%) or a depolarization (n = 15; 7%) of mitral cells, the two types of response being observed in two distinct subsets. OXA-induced hyperpolarizations were long lasting and of small amplitudes. At 100 nM, hyperpolarizations had a 3 ± 2 mV mean amplitude that occurred after a 30 ± 9.5 sec delay and lasted 95 ± 57 sec. In spontaneously active cells (n = 12), these hyperpolarizations caused a complete cessation of spontaneous spikes or excitatory postsynaptic potentials (EPSP; Fig. 5, A and B).

OXA-induced hyperpolarizations were reproducible in cells that were tested with successive applications (n = 3, data not shown) and were abolished if TTX, the fast Na^+ channel blocker, was added to the ACSF (n = 2; Fig. 6, A and B). In Fig. 6, C and D, it can be seen that OXA caused a cessation of spontaneous firing in the control, whereas in the presence of bicuculline, it only slowed down spontaneous firing. Bicuculline decreased the amplitude of OXA hyperpolarizing responses by 17–75% (n = 14). Picrotoxin (n = 5) had similar effects to bicuculline (data not shown). When the

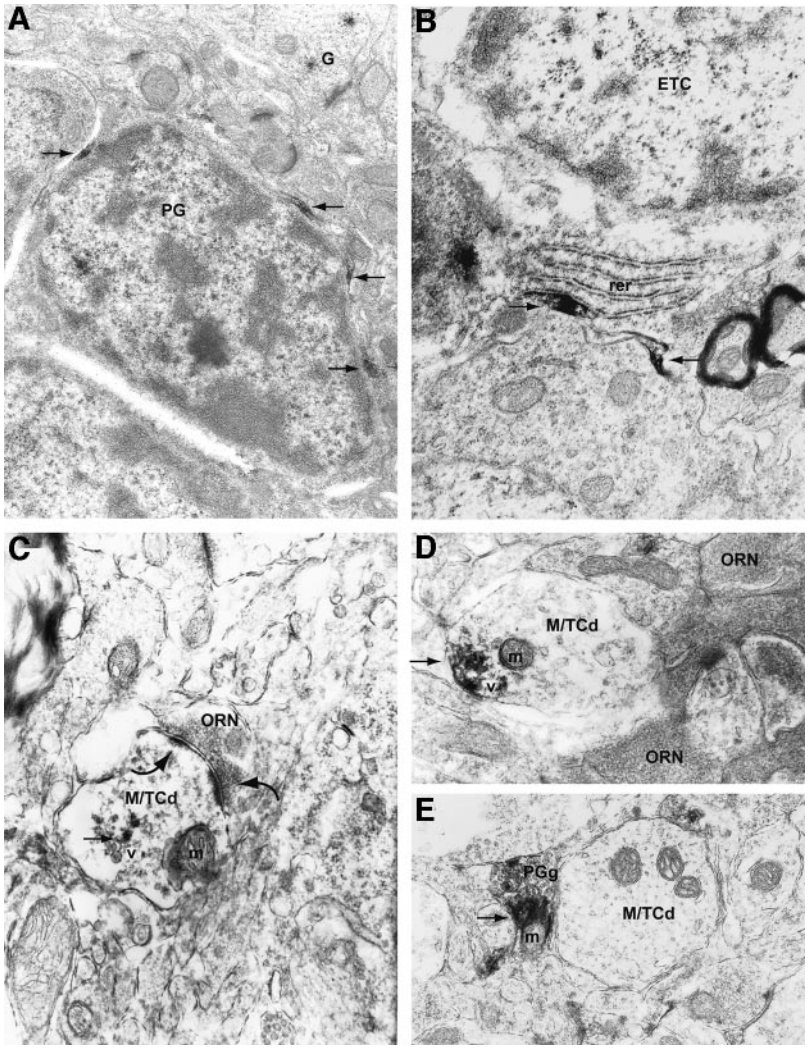

FIG. 4. Ultrastructural localization of ORX1 in the glomerular layer of the OB. At the ultrastructural level, the presence of ORX1 was visualized by electron-dense DAB deposits (*arrows*). In the glomerular layer (A, ×12,000), DAB electron-dense deposits (*arrows*) were found in small cells exhibiting a large nucleus surrounded by a thin rim of cytoplasm. These cells, located around the glomeruli, were identified as PGs. At the basis of glomeruli (infraglomerular layer area, B, ×19,000), some larger cells characterized by stacks of rer were also ORX1 immunoreactive. These ultrastructural characteristics correspond to those of external tuft cell. In the glomerular neuropile (C, ×28,000; D, ×29,000), ORX1 immunoreactive dendrites of mitral/tufted cells are numerous and were surrounded by ORN terminals, showing synaptic contacts (C, *curved arrows*). Some gemmules (kind of typical varicosities as termed by OB anatomists; see Ref. 39) of PGs were also ORX1 immunoreactive (E, ×17,000). ETC, External tufted cell; G, glomerulus; m, mitochondria; M/TCd, mitral/tufted cell dendrite; ORN, olfactory receptor neuron; rer, rough endoplasmic reticulum; v, synaptic vesicles; PGg, gemmule of periglomerular cell.

ACSF perfusion contained SB-334867-A (ORX1 antagonist), hyperpolarizing responses were completely blocked (n = 4; Fig. 7, A and B). Altogether the results indicate that the hyperpolarizing effect of OXA is an indirect effect. OXA may act through ORX1 on GABAergic neurons that would act in turn on mitral cell $GABA_A$ receptors. Consistent with this hypothesis, bicuculline decreased the OXA hyperpolarizing effect in mitral cells.

In a distinct set of 14 mitral cells, bath application of OXA-induced long-lasting small-amplitude depolarizations (Fig. 8A). At 25 nM, OXA depolarizations had a 2 ± 0.6 mV mean amplitude, occurred after a 33 ± 18-sec delay, and lasted 241 ± 84 sec. Orexin depolarizations were insensitive to TTX (n = 2; Fig. 8B). To examine this depolarizing effect in detail, subsequent experiments were conducted under voltage-clamp conditions. When the membrane potential was voltage clamped at, or near, its resting level, OXA produced an inward current whose delay and duration matched those of the OXA-induced depolarizations (Fig. 9A). This inward current was blocked by SB-334867-A (n = 3; Fig. 9B). These experiments indicate that the OXA depolarizing action on mitral cells is direct and mediated through ORX1.

Among the 46 mitral cells hyperpolarized by OXA, 42 were submitted to electrical stimulation applied on olfactory nerves (complete protocol is described in Ref. 33); 21 mitral cells were responsive to this stimulation. For each recorded cell, the excitation threshold was determined in control condition, and the stimulation intensity was adjusted to elicit one spike per shock with a stable latency. Then OXA was perfused into the recording chamber, and its effect on mitral cell response parameters (threshold, latency, and number of spikes) was analyzed as a function of time. In four mitral cells, olfactory nerve stimulation excitability was decreased by OXA (Fig. 10), although it was not affected in 17.

Discussion

Past studies have shown orexin fibers and receptors in the adult rat OB (9–13, 31). However, until now, no data about the development of orexin innervation and orexin receptor expression were available in this tissue. Through RT-PCR experiments, we present information of orexin receptor mRNA in the OB during early postnatal development. Our results indicate that both ORX1 and ORX2 are expressed as early as 10 d after birth (P10) and their presence is shown until the adult stage both in control tissues (HYPO) and OB.

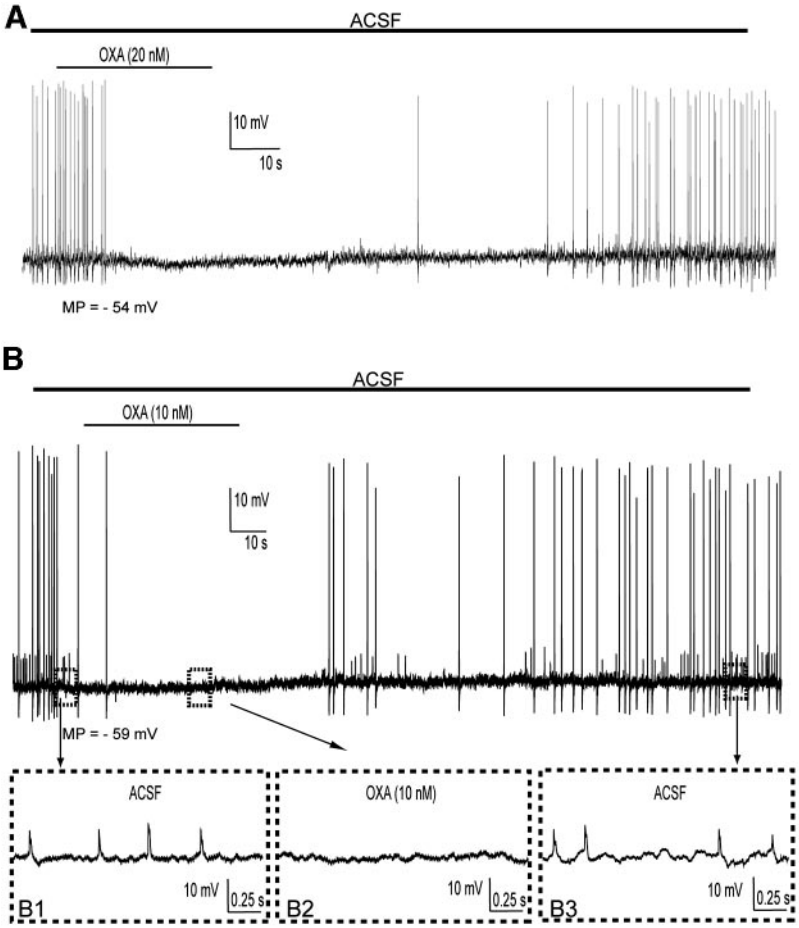

FIG. 5. Inhibitory action of OXA on mitral cells. A, 20 nM OXA (*horizontal bar*) totally abolished mitral cell spontaneous activity; control activity recovered after a rinsing period of 120 sec. B, Mitral cell showing spontaneous activity composed of spikes and EPSPs, which were both abolished by OXA (10 nM). B1–B3, Enlargement of 2-sec periods focusing on EPSPs. B1, Spontaneous EPSPs in control. B2, Disappearance of EPSPs under OXA. B3, Recovery of spontaneous EPSPs after rinsing. MP, Resting membrane potential at the beginning of the recording.

Although only a quantitative RT-PCR could lead us to a more definitive conclusion, our study suggests that both ORX1 and ORX2 are expressed at a lower level in OB, compared with HYPO. Noteworthy is that our results show a stable level of ORX1 expression before weaning as well as in adults. Other brain tissues, such as hypoglossal neurons (42) or hypothalamus (43), show higher expression levels at P20–25 and a stable level thereafter. From a functional point of view, Van den Pol *et al.* (44) report that the orexin system is functional during early brain development and show that at P10, orexin induces a robust synaptic activity in hypothalamic neurons. Altogether our results and those on hypothalamic structures convinced us to perform our electrophysiological recordings on P10–25 rats.

Furthermore, from our anatomical results, it appears that the cellular localization of ORX1 is similar in preweaning and adult rats. At light microscopic level, our immunocytochemical study confirms the localization of ORX1 in mitral/tufted cell bodies reported by Caillol *et al.* (31). At the ultrastructural level, the localization of orexin receptors has been not widely studied; there is only one recent publication in the arcuate nucleus (45). Our results are in agreement with this study showing that ORX1 was localized in cell bodies as well as at the pre- and postsynaptic levels. In our study, a part of the labeling is localized in the rough endoplasmic reticulum, suggesting a local synthesis of ORX1. ORX1 immunoreactivity was also shown in mitral/tufted cell dendrites running in the EPL and in bodies and processes of external tuft cells and periglomerular and granule cells. Thus, ORX1 seems to be expressed by most OB cell categories but not in a systematic and homogeneous way. Indeed, ORX1 labeling is homogeneously distributed neither along the mitral cell layer nor in the glomerular layer. Interestingly, ORX1 immunoreactive mitral cell bodies were found in most cases adjacent to ORX1 immunoreactive glomeruli. Although such an observation needs to be further documented, it may suggest some columnar organization of orexin receptive cells in the OB.

To optimize *in vitro* neuron survival, electrophysiological recordings were performed on 10- to 25-d-old rats, a period surrounding weaning. During this period, ingestive behavior evolves: the type of food changes from a liquid diet full of fat to a solid diet with less fat. However, in our experimental conditions, we observed that weaning is progressive because developing rats can both suck at their mothers' nipples and eat solid food, which is available *ad libitum* (for the dam). Furthermore, most of recordings (75%) were made from 20- to 25-d-old rats, and no obvious variability due to different ages of rats was observed in mitral cell reactivity to OXA.

Our results show that OXA modulates mitral cell activity. Only 61 mitral cells (30%) were shown to be modulated by OXA, with 7 and 23% being depolarized and hyperpolarized, respectively. These results are in agreement with our immu-

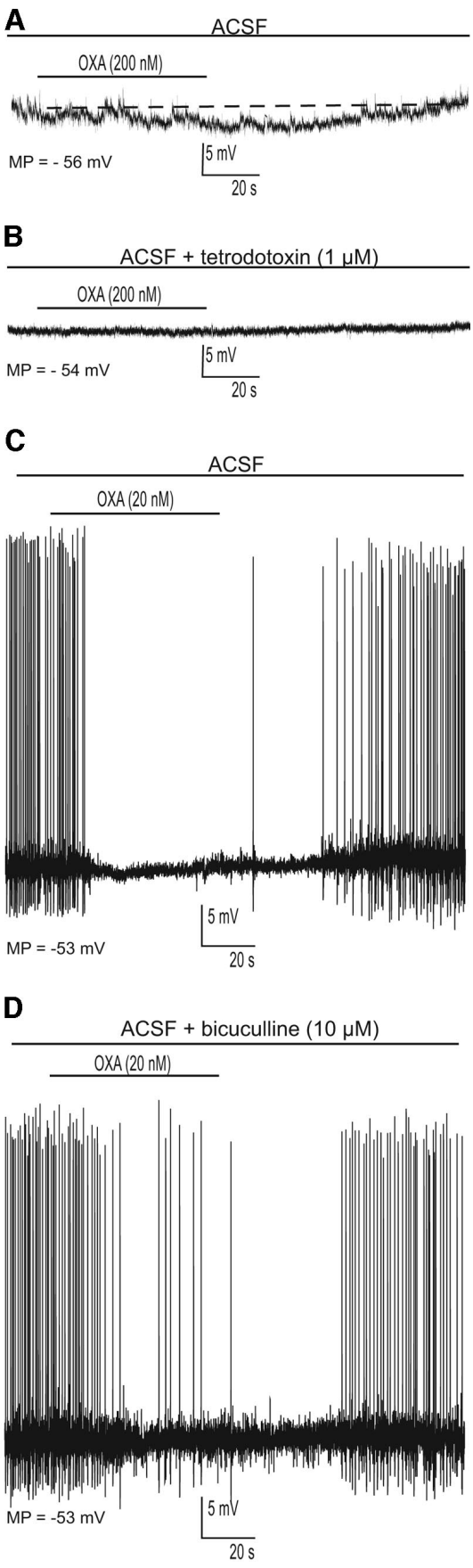

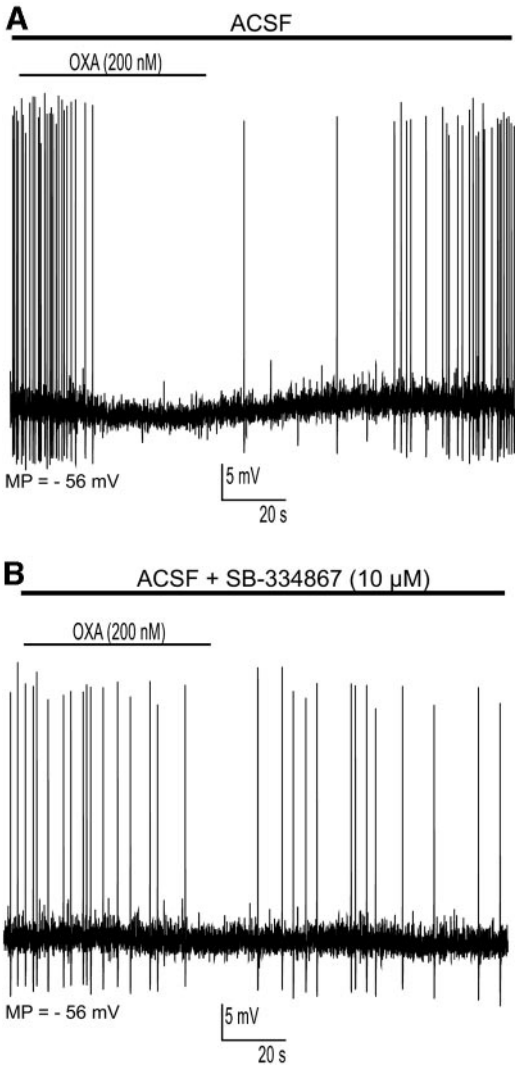

FIG. 7. Characterization of orexin receptor type involved in mitral cell hyperpolarizing responses. A, OXA (200 nM) hyperpolarized a mitral cell in control condition. B, SB-334867 (ORX1 antagonist, 10 μM) blocked completely the OXA-induced hyperpolarization. MP, Resting membrane potential at the beginning of the recording.

nocytochemical observations, which indicate that rather few mitral cells were ORX1 immunoreactive.

OXA is shown to exert two opposite effects on two distinct sets of mitral cells: either a direct depolarizing effect, by inducing a TTX-insensitive inward current, or an indirect hyperpolarizing effect. However, both OXA effects were blocked by SB-334867-A, which demonstrated the involvement of ORX1 (Fig. 11).

The hyperpolarizing action of OXA was sufficient to completely shut off mitral cell spontaneous activity and was antagonized by the voltage-gated Na^+ channel blocker TTX.

FIG. 6. Inhibitory action of OXA may be indirect. A, OXA (200 nM) hyperpolarized a silent mitral cell. B, The hyperpolarizing effect of OXA was abolished by TTX (1 μM). C, OXA (20 nM) hyperpolarized a spontaneously active mitral cell by 1.5 mV; *horizontal scale bar*, 20 sec; *vertical scale bar*, 5 mV. D, The hyperpolarizing effect of OXA was maintained under bicuculline (10 μM) but reduced to about 0.5 mV. MP, Resting membrane potential at the beginning of the recording.

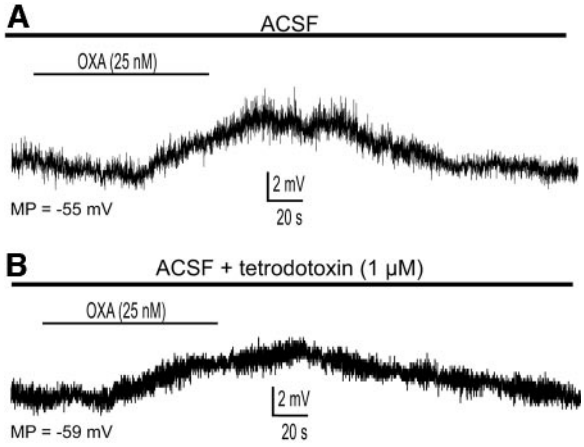

FIG. 8. OXA depolarizes mitral cell. A, OXA (25 nM) depolarized a mitral cell by 4 mV. B, This depolarization was not prevented by TTX. MP, Resting membrane potential at the beginning of the recording.

The latter observation supports that OXA action was indirect. Such OXA indirect effects were reported in other brain area like the substantia nigra (34), laterodorsal tegmental nucleus (46), HYPO (47), or raphe nucleus (43). These OXA effects were either excitatory or inhibitory.

We show that the OXA hyperpolarizing response was partly antagonized by the $GABA_A$ receptor antagonist, bicuculline. This result indicates that GABAergic interneurons are involved in the OXA-induced hyperpolarization of mitral cells. Our immunocytochemical observations that some PG and granule cell bodies express ORX1 support that these GABAergic interneurons could be contacted by orexin fibers localized mainly in glomerular layer and feebly in granule cell layer (31). Indeed, PG and granule cells, the main interneurons of these two layers, are mainly GABAergic (49, 50) and have been shown to inhibit mitral cells by activation of $GABA_A$ receptors (51, 52). Along the same line, GABAergic interneurons that are excited by OXA may act on metabotropic $GABA_B$ receptors. Indeed, $GABA_B$ receptor activation was reported elsewhere to both abolish completely spontaneous activity in mitral cells and decrease mitral cell excitability to electrical shocks applied in the olfactory nerve layer (33, 53, 54).

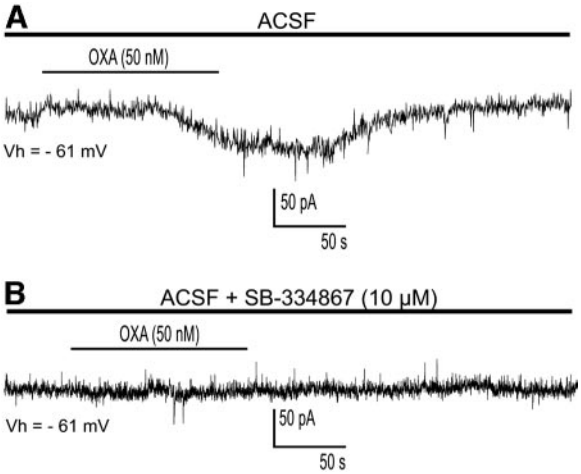

FIG. 9. ORX1 is involved in OXA-induced inward current. A, OXA induced a slow inward current. B, SB-334867 (10 μM) abolished this current. Vh, Holding potential; MP, resting membrane potential at the beginning of the recording.

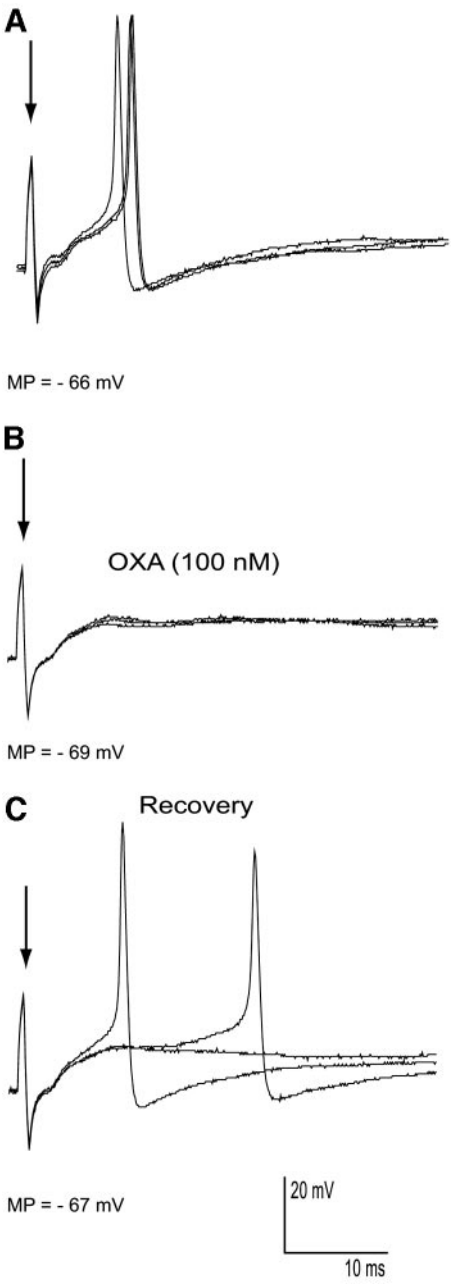

FIG. 10. Effect of OXA on mitral cell responses evoked by olfactory nerve stimulation. A, Three superimposed control responses to olfactory nerve stimulation, one spike per stimulation. B, Five minutes after a perfusion of a 100 nM OXA solution, which hyperpolarized the cell to −69 mV, stimulations failed to induce action potential. C, Partial recovery of control excitability (two spikes for three stimulations) was obtained after a rinsing period of 10 min. MP, Resting membrane potential at the beginning of the recording.

In the present study, OXA was also observed to decrease mitral cell excitability to electrical shocks. For such an effect, OXA-induced GABA-release may act on extrasynaptic presynaptic $GABA_B$ receptors located on primary afferent axons (55, 56) in which it is strongly suspected to act by depressing

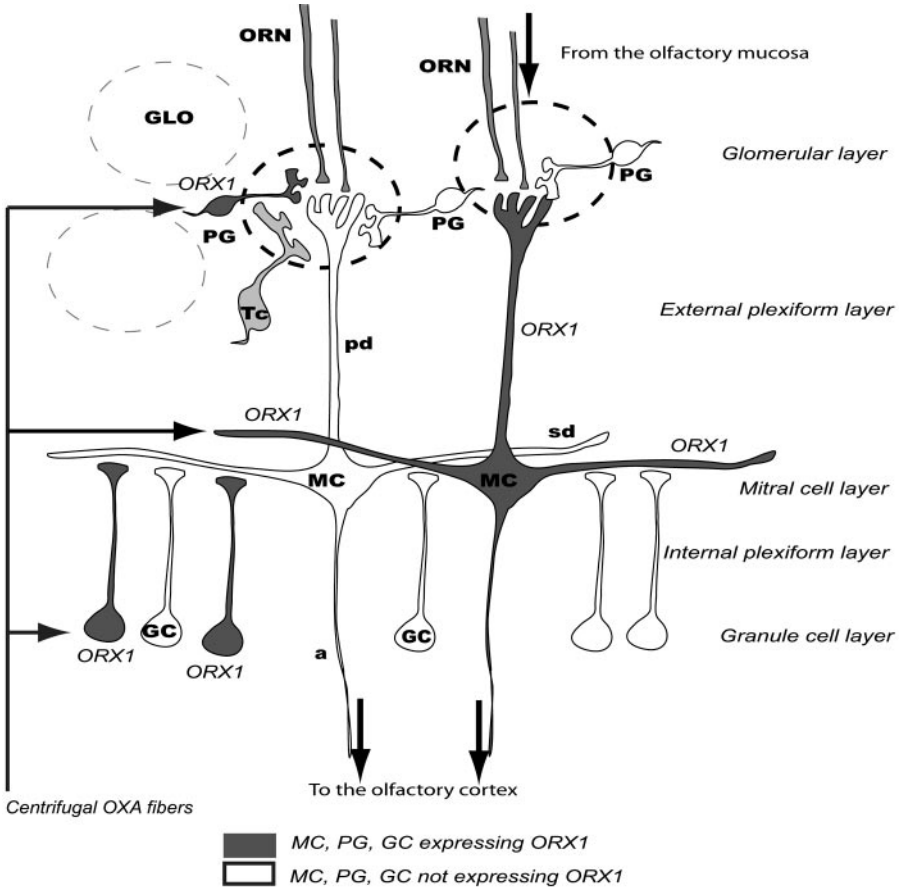

FIG. 11. OXA action on mitral cells in the rat OB network. From the olfactory mucosa, olfactory receptor neurons (ORN) send their axons to the OB terminating in glomeruli (GLO), spherical neuropiles lying at the OB periphery. Within glomeruli, these axons synapse with primary dendrites (pd) of mitral cells (MC). Mitral cells make reciprocal dendrodendritic synapses with the two categories of GABAergic inhibitory interneurons; through their pd with PGs and through their secondary dendrites (sd) with granule cells (GC). So mitral cell activity can be modulated through a double-GABAergic control before sending their axon (a) to the olfactory cortex. ORX1 is found to be expressed by subsets of MC, PG, and GC (cells in *dark gray*) and tufted cells (Tc, in *light gray*), these receptors being localized in the soma and processes of these neurons. *Left*, The diagram schematizes the indirect hyperpolarizing action of OXA on MC: OXA, by acting through ORX1, is hypothesized to depolarize GABAergic inhibitory interneurons, PGs, or GCs (in *dark gray*), which in turn would inhibit MCs (in *white*) via a GABA release acting on GABAA receptors localized on the MC. Within glomeruli, a part of OXA indirect hyperpolarizing action can also be ascribed to action of GABA released by PGs on GABAB receptors localized both on ORN axons or MCs (pd). *Right*, The diagram is schematizes the direct depolarizing action of OXA on MC; OXA, by acting through ORX1 expressed by a subset of mitral cells, is hypothesized to depolarize MC (*dark gray*).

neurotransmitter release (54, 57–60). On the other hand, for decreasing mitral cell spontaneous activity, OXA-induced GABA-release may act on $GABA_B$ receptors located either on the soma or dendritic intraglomerular tuft of rat mitral cells (55, 56). One of the mechanisms by which $GABA_B$ would silence the spontaneous activity may be that $GABA_B$ would slightly hyperpolarize mitral cells at rest, shifting the cell polarization from the up-state to the down-state, the latter signaling a steady silent state (61). Because dopamine and GABA are colocalized in some PG interneurons (62–64), dopamine also would be a good candidate to support the OXA indirect inhibition of mitral cells. Consistent with this hypothesis is that, in the frog OB, dopamine was found to inhibit mitral cell spontaneous activity (65). A coaction of GABA and dopamine cannot be ruled out.

An especially interesting fact is that our electrophysiological results are fully consistent with those of an *in vivo* study (48). The authors recorded unit extracellular activity of mitral cells in anesthetized rats, whereas they applied OXA directly on the OB surface or in the lateral ventricle. Both types of applications were shown to induce a decrease in spontaneous rate of some cells or an increase in others distinct cells. Noteworthy is that in both *in vivo* and *in vitro* studies, OXA induces two types of opposite actions on mitral cell spontaneous activity.

As a conclusion, our study brings out information on the ontogenetic expression of orexin receptors in the rat OB and clarifies ORX1 structural and ultrastructural localization within the network. In addition, our *in vitro* recordings demonstrate that OXA acts on mitral cells both directly and indirectly inducing apparently opposite effects. The direct depolarizing effect could be mediated by ORX1 located on mitral cell bodies and dendrites. ORX1 located on PG and granular cells could be responsible for the indirect hyperpolarizing action of OXA via GABA-induced release.

Altogether our data provide new insights for apprehending some of the mechanisms by which the olfactory system is involved in the regulation of food-intake behavior. In hungry animals, hypothalamic OX neurons are stimulated by hypoglycemia (14) and probably increase their release through centrifugal pathways. Our electrophysiological data detail OX action in OB. Indeed, by acting both directly by increasing output neuron's background activity and, indirectly through inhibitory interneuron networks, OX can both depress and excite mitral cells. These two opposite actions are shown to occur in two distinct mitral cell sets. OX may provide for selective and dual actions in olfactory information processing, favoring mitral cells involved in the food-odor processing and silencing others that are not involved. This duality of action could result in increasing signal to noise ratio and may increase olfactory detection power. This hypothesis fully agrees with behavioral experiments, which are in progress by our research team. Indeed, preliminary results indicate that olfactory detection thresholds of rats are enhanced by OXA intracerebral injection.

Acknowledgments

We thank GlaxoSmithKline (Harlow, Essex, UK) for their generous gift of SB-334867-A and Professor Edwin Griff (University of Cincinnati, Cincinnati, OH) for careful reading in English.

Received January 11, 2005. Accepted June 8, 2005.

Address all correspondence and requests for reprints to: Patricia Duchamp-Viret, Laboratoire de Neurosciences et Systèmes Sensoriels, Centre National de la Recherche Scientifique, Unité Mixte de Recherche 5020, Université Claude Bernard, 50 Avenue Tony Garnier, 69366 Lyon cedex 07, France. E-mail: pduchamp@olfac.univ-lyon1.fr.

References

1. **Chaput M, Holley A** 1976 Olfactory bulb responsiveness to food odour during stomach distension in the rat. Chem Senses 2:198–201
2. **Pager J** 1974 A selective modulation of olfactory input suppressed by lesions of the anterior limb of the anterior commisure. Physiol Behav 13:523–526
3. **Pager J** 1974 A selective modulation of the olfactory bulb electrical activity in relation to the learning of palatability in hungry and satiated rats. Physiol Behav 12:189–195
4. **Pager J** 1978 Ascending olfactory information and centrifugal influxes contributing to a nutritional modification of the rat mitral cell responses. Brain Res 140:251–271
5. **Pager J, Giachetti I, Holley A, Le Magnen J** 1972 A selective control of olfactory bulb electrical activity in relation to food deprivation and satiety in rats. Physiol Behav 9:573–579
6. **Giachetti I, Mac Leod P, Le Magnen J** 1970 Influence of hunger and satiety states on responses of the olfactory bulb in rats. J Physiol (Paris) 62(Suppl 2):280–281
7. **Le Magnen J** 1999 Increased food intake induced in rats by changes in the satiating sensory input from food (first published in French in 1956). Appetite 33:33–35
8. **Bernardis LL, Bellinger LL** 1996 The lateral hypothalamic area revisited: ingestive behavior. Neurosci Biobehav Rev 20:189–287
9. **Chemelli RM, Willie JT, Sinton CM, Elmquist JK, Scammell T, Lee C, Richardson JA, Williams SC, Xiong Y, Kisanuki Y, Fitch TE, Nakazato M, Hammer RE, Saper CB, Yanagisawa M** 1999 Narcolepsy in orexin knockout mice: molecular genetics of sleep regulation. Cell 98:437–451
10. **Date Y, Ueta Y, Yamashita H, Yamaguchi H, Matsukara S, Kangawa K, Sakurai T, Yanagisawa M, Nakazato M** 1999 Orexins, orexigenic hypothalamic peptides, interact with autonomic, neuroendocrine and neuroregulatory systems. Proc Natl Acad Sci USA 96:748–753
11. **De Lecea L, Kilduff TS, Peyron C, Gao X, Foye PE, Danielson PE, Fukuhara C, Battenberg EL, Gautvik VT, Bartlett 2nd FS, Frankel WN, van den Pol AN, Bloom FE, Gautvik KM, Sutcliffe JG** 1998 The hypocretins: hypothalamus-specific peptides with neuroexcitatory activity. Proc Natl Acad Sci USA 95: 322–327
12. **Peyron C, Tighe D, Vanden Pol AN, De Lecea L, Heller HC, Sutcliffe JG, Kilduff TS** 1998 Neurons containing hypocretin (orexin) project to multiple neuronal systems. J Neurosci 18:9996–10015
13. **Sakurai T, Amemiya A, Ishii M, Matsuzaki I, Chemelli RM, Tanaka H, Williams SC, Richarson JA, Kozlowski GP, Wilson S, Arch JR, Buckingham RE, Haynes AC, Carr SA, Annan RS, McNulty DE, Liu WS, Terrett JA, Elshourbagy NA, Bergsma DJ, Yanagisawa M** 1998 Orexins and orexin receptors: a family of hypothalamic neuropeptides and G protein-coupled receptors that regulate feeding behavior. Cell 92:696
14. **Moriguchi T, Sakurai T, Nambu T, Yanagisawa M, Goto K** 1999 Neurons containing orexin in the lateral hypothalamic area of the adult rat brain are activated by insulin-induced acute hypoglycemia. Neurosci Lett 264:101–104
15. **Griffond B, Risold PY, Jacquemard C, Colard C, Fellmann D** 1999 Insulin-induced hypoglycemia increases preprohypocretin (orexin) mRNA in the rat lateral hypothalamic area. Neurosci Lett 262:77–80
16. **Briski KP, Sylvester PW** 2001 Hypothalamic orexin-A-immunopositive neurons express Fos in response to central glucopenia. Neuroreport 12:531–534
17. **Cai XJ, Denis R, Vernon RG, Clapham JC, Wilson S, Arch JR, Williams G** 2001 Food restriction selectively increases hypothalamic orexin-B levels in lactating rats. Regul Pept 97:163–168
18. **Cai XJ, Widdowson PS, Harrold J, Wilson S, Buckingham RE, Arch JR, Tadayyon M, Clapham JC, Wilding J, Williams G** 1999 Hypothalamic orexin expression: modulation by blood glucose and feeding. Diabetes 48:2132–2137
19. **Yamanaka A, Muraki Y, Tsujino N, Goto K, Sakurai T** 2003 Regulation of orexin neurons by the monoaminergic and cholinergic systems. Biochem Biophys Res Commun 303:120–129
20. **Bahjaoui-Bouhaddi M, Fellmann D, Griffond B, Bugnon C** 1994 Insulin treatment stimulates the rat melanin-concentrating hormone-producing neurons. Neuropeptides 27:251–258
21. **Wortley KE, Chang GQ, Davydova Z, Leibowitz SF** 2003 Peptides that regulate food intake: orexin gene expression is increased during states of hypertriglyceridemia. Am J Physiol Regul Integr Comp Physiol 284:R1454–R1465
22. **Hagan JJ, Leslie RA, Patel S, Evans ML, Wattam TA, Holmes S, Benham CD, Taylor SG, Routledge C, Hemmati P, Munton RP, Ashmeade TE, Shah AS, Hatcher JP, Hatcher PD, Jones DN, Smith MI, Piper DC, Hunter AJ, Porter RA, Upton N** 1999 Orexin A activates locus coeruleus cell firing and increases arousal in the rat. Proc Natl Acad Sci USA 96:10911–10916
23. **Ida T, Nakahara K, Katayama T, Murakami N, Nakazato M** 1999 Effect of lateral cerebroventricular injection of the appetite-stimulating neuropeptide, orexin and neuropeptide Y, on the various behavioral activities of rats. Brain Res 821:526–529
24. **Leibowitz SF, Wortley KE** 2004 Hypothalamic control of energy balance: different peptides, different functions. Peptides 25:473–504
25. **Rodgers RJ, Ishii Y, Halford JC, Blundell JE** 2002 Orexins and appetite regulation. Neuropeptides 36:303–325
26. **Edwards CM, Abusnana S, Sunter D, Murphy KG, Ghatei MA, Bloom SR** 1999 The effect of the orexins on food intake: comparison with neuropeptide Y, melanin-concentrating hormone and galanin. J Endocrinol 160:R7–R12
27. **Lubkin M, Stricker-Krongrad A** 1998 Independent feeding and metabolic actions of orexins in mice. Biochem Biophys Res Commun 253:241–245
28. **Mondal MS, Nakazato M, Matsukura S** 2000 Orexins (hypocretins): novel hypothalamic peptides with divergent functions. Biochem Cell Biol 78:299–305
29. **Smart D, Jerman JC, Brough SJ, Neville WA, Jewitt F, Porter RA** 2000 The hypocretins are weak agonists at recombinant human orexin-1 and orexin-2 receptors. Br J Pharmacol 129:1289–1291
30. **Smart D, Jerman JC, Brough SJ, Rushton SL, Murdock PR, Jewitt F, Elshourbagy NA, Ellis CE, Middlemiss DN, Brown F** 1999 Characterization of recombinant human orexin receptor pharmacology in a Chinese hamster ovary cell-line using FLIPR. Br J Pharmacol 128:1–3
31. **Caillol M, Aioun J, Baly C, Persuy MA, Salesse R** 2003 Localization of orexins and their receptors in the rat olfactory system: possible modulation of olfactory perception by a neuropeptide synthetized centrally or locally. Brain Res 960: 48–61
32. **Chomczynski P, Sacchi N** 1987 Single-step method of RNA isolation by acid guanidinium thiocyanate-phenol-chloroform extraction. Anal Biochem 162: 156–159
33. **Palouzier-Paulignan B, Duchamp-Viret P, Hardy AB, Duchamp A** 2002 $GABA_B$ mediated inhibition of mitral cell activity in the rat olfactory bulb: a whole-cell patch clamp study *in vitro*. Neuroscience 111:241–250
34. **Korotkova TM, Eriksson KS, Haas HL, Brown RE** 2002 Selective excitation of GABAergic neurons in the substantia nigra of the rat by orexin/hypocretin *in vitro*. Regul Pept 104:83–89
35. **Korotkova TM, Sergeeva OA, Eriksson KS, Haas HL, Brown RE** 2003 Excitation of ventral tegmental area dopaminergic and nondopaminergic neurons by orexins/hypocretins. J Neurosci 23:7–11
36. **Yang B, Ferguson AV** 2002 Orexin-A depolarizes dissociated rat area postrema neurons through activation of a nonselective cationic conductance. J Neurosci 22:6303–6308
37. **Soffin EM, Evans ML, Gill CH, Harries MH, Benham CD, Davies CH** 2002 SB-334867-A antagonises orexin mediated excitation in the locus coeruleus. Neuropharmacology 42:127–133
38. **Matsuo K, Kaibara M, Uezono Y, Hayashi H, Taniyama K, Nakane Y** 2002 Involvement of cholinergic neurons in orexin-induced contraction of guinea pig ileum. Eur J Pharmacol 452:105–109
39. **Pinching AJ, Powell TPS** 1971 The neuron types of the glomerular layer of the olfactory bulb. J Cell Sci 9:305–345
40. **Pinching AJ, Powell TPS** 1971 The neuropil of the periglomerular region of the olfactory bulb. J Cell Sci 9:379–409
41. **Price JL, Powell TPS** 1970 The synaptology of the granule cells of the olfactory bulb. J Cell Sci 7:125–155
42. **Volgin DV, Saghir M, Kubin L** 2002 Developmental changes in the orexin 2 receptor mRNA in hypoglossal motoneurons. Neuroreport 13:433–436
43. **Liu RJ, van den Pol AN, Aghajanian GK** 2002 Hypocretins (orexins) regulate serotonin neurons in the dorsal raphe nucleus by excitatory direct and inhibitory indirect actions. J Neurosci 22:9453–9464
44. **Van den Pol AN, Patrylo PR, Ghosh PK, Gao XB** 2001 Lateral hypothalamus: early developmental expression and response to hypocretin (orexin). J Comp Neurol 433:349–363
45. **Guan XB, Suzuki R, Funahashi H, Wang QP, Kageyama H, Uehara K, Yamada S, Tsurugano S, Shioda S** 2002 Ultrastructural localization of orexin-1 receptor in pre- and post-synaptic neurones in the rat arcuate nucleus. Neurosci Lett 329:209–212
46. **Burlet S, Tyler CJ, Leonard CS** 2002 Direct and indirect excitation of laterodorsal tegmental neurons by hypocretin/orexin peptides: implications for wakefulness and narcolepsy. J Neurosci 22:2862–2872
47. **Follwell MJ, Ferguson AV** 2002 Cellular mechanisms of orexin actions on paraventricular nucleus neurones in rat hypothalamus. J Physiol 545:855–867
48. **Apelbaum A, Perrut A, Chaput M** 2005 Orexin A effects on the olfactory bulb spontaneous activity and odor responsiveness in freely breathing rats. Regul Pept 129:49–61
49. **Mugnaini E, Oertel WH, Wouterlood FF** 1984 Immunocytochemical localization of GABA neurons and dopamine neurons in the rat main and accessory olfactory bulbs. Neurosci Lett 47:221–226

50. **Ribak CE, Vaughn JE, Saito K, Barber B, Roberts E** 1977 Glutamate decarboxylase localization in neurons of the olfactory bulb. Brain Res 126:1–18
51. **Duchamp-Viret P, Duchamp A, Chaput M** 1993 GABAergic control of odor-induced activity in the frog olfactory bulb—electrophysiological study with picrotoxin and bicuculline. Neuroscience 53:111–120
52. **Jahr CE, Nicoll RA** 1982 An intracellular analysis of dendrodendritic inhibition in the turtle *in vitro* olfactory bulb. J Physiol 326:213–234
53. **Duchamp-Viret P, Delaleu JC, Duchamp A**. 2000 GABA(B)-mediated action in the frog olfactory bulb makes odor responses more salient. Neuroscience 97:771–777
54. **Nickell WT, Behbehani MM, Shipley MT** 1994 Evidence for GABA(B)-mediated inhibition of transmission from the olfactory nerve to mitral cells in the rat olfactory bulb. Brain Res Bull 35:119–123
55. **Bonino M, Cantino D, Sassoe-Pognetto M** 1999 Cellular and subcellular localization of γ-aminobutyric acid (B) receptors in the rat olfactory bulb. Neuroscience Letters 274:195–198
56. **Margeta-Mitrovic M, Mitrovic I, Riley RC, Jan LY, Basbaum AI** 1999 Immunohistochemical localization of GABA(B) receptors in the rat central nervous system. J Comp Neurol 405:299–321
57. **Aroniadou-Anderjaska V, Zhou F.-M., Priest CA, Ennis M, Shipley MT** 2000 Tonic and synaptically evoked presynaptic inhibition of sensroy input to the rat olfactory bulb via $GABA_B$ heteroreceptors. J Neurophysiol 84:1194–1203
58. **Potapov AA** 1985 Baclofen inhibition of synaptic transmission in the frog olfactory glomeruli. Neirofiziologiya 17:834–837
59. **Potapov AA, Trepakov VV** 1986 Two types of GABA receptors in the intact olfactory bulb and primordial hippocampus of the frog: pharmacological data. Bull Exp Biol Med 101:323–326
60. **Wachowiak M, Cohen LB** 1999 Presynaptic inhibition of primary olfactory afferents mediated by different mechanisms in lobster and turtle. J Neurosci 19:8808–8817
61. **Heyward P, Ennis M, Keller A, Shipley MT** 2001 Membrane bistability in olfactory bulb mitral cells. J Neurosci 21:5311–5320
62. **Gall C, Hendry SHC, Seroogy KB, Jones EG, Haycock JW** 1987 Evidence for coexistence of GABA and dopamine in neurons of the rat olfactory bulb. J Comp Neurol 266:307–318
63. **Kosaka K, Toida K, Margolis FL, Kosaka T** 1997 Chemically defined neuron groups and their subpopulations in the glomerular layer of the rat main olfactory bulb. 2. Prominent differences in the intraglomerular dendritic arborization and their relationship to olfactory nerve terminals. Neuroscience 76:775–786
64. **Kosaka T, Hataguchi Y, Hama K, Nagatsu I, Wu JY** 1985 Coexistence of immunoreactivities for glutamate decarboxylase and tyrosine hydroxylase in some neurons in the periglomerular region of the rat main olfactory bulb: possible coexistence of γ-aminobutyric acid (GABA) and dopamine. Brain Res 343:166–171
65. **Duchamp-Viret P, Coronas V, Delaleu JC, Moyse E, Duchamp A** 1997 Dopaminergic modulation of mitral cell activity in the frog olfactory bulb: a combined radioligand binding electrophysiological study. Neuroscience 79:203–216

***Endocrinology* is published monthly by The Endocrine Society (http://www.endo-society.org), the foremost professional society serving the endocrine community.**